*Journal of Alloys and Compounds, 182* (1992) 233–242
*JALCOM 168*



# A study of Pr–Fe–B–Cu permanent magnetic alloys

H. W. Kwon, P. Bowen and I. R. Harris
*School of Metallurgy and Materials, The University of Birmingham, Birmingham B15 2TT (UK)*

(Received October 22, 1991)

## Abstract

The microstructures and magnetic properties of alloys $Pr_{20.5}Fe_{74.0}B_{3.5}Cu_{2.0}$ (A) and $Pr_{17.0}Fe_{76.5}B_{5.0}Cu_{1.5}$ (B) have been investigated. In the cast condition the microstructure of alloy A consisted of three phases: a $Pr_2Fe_{14}B$ matrix phase, a praseodymium-rich grain boundary phase and free iron inside the matrix phase. Little of the $PrFe_4B_4$ (approximate composition) boride phase which is frequently observed in RE–Fe–B-type alloys (RE, rare earth) was observed in alloy A. The microstructure of alloy B in the cast state consisted of four phases: the same three phases as those observed in alloy A together with the $PrFe_4B_4$ phase. A greater amount of the grain boundary phase and a smaller grain size were observed in alloy A compared with alloy B. In annealed (1000 °C for 5 h) and slowly cooled alloy A an extra phase with needle-like or irregular form was observed in the grain boundary region. The ratio Pr:Fe in the extra phase was analysed to be about 1:2 and this phase was suggested to be a $PrFe_2$-type phase ($Pr(Fe_{0.94}Cu_{0.06})_2$). In alloy B the microstructure was not altered radically by annealing except for the disappearance of the free iron. Alloy A exhibited much better permanent magnetic properties than alloy B and this was attributed to the smaller grain size and improved magnetic isolation of the individual grains. The effects of low temperature annealing on the magnetic properties at 500 °C have also been investigated.

## 1. Introduction

Praseodymium is very similar to neodymium in the elemental state and in $RE_2Fe_{14}B$-type compounds (RE, rare earth). However, in $Nd_2Fe_{14}B$ a conical spin reorientation occurs at around 135 K [1], whereas $Pr_2Fe_{14}B$ exhibits no spin reorientation down to 4.2 K [2] and has a higher anisotropy field [3] than $Nd_2Fe_{14}B$. Thus at low temperatures $Pr_2Fe_{14}B$ exhibits much smaller variations in the magnetic properties than $Nd_2Fe_{14}B$. It has been suggested [4], therefore, that magnets based on $Pr_2Fe_{14}B$ can be employed for low temperature applications. The hard magnetic properties of RE–Fe–B alloys are generally fairly poor in the cast state. Recently, however, it has been found [5–8] that the Pr–Fe–B-based alloys can exhibit appreciable coercivity even in the bulk ingot state by employing a proper heat treatment and the minor addition of elements such as copper, aluminium and silver. In this paper a detailed study of the microstructure and magnetic properties of two Pr–Fe–B-based alloys was carried out as a precursor to a study of the effects of high temperature mechanical deformation on these materials. A substantially

0925-8388/92/$5.00

praseodymium-rich alloy (A) was selected in order to increase the amount of praseodymium-rich material and hence facilitate the metallographic examination of the grain boundary regions and improve the magnetic isolation of the individual grains. The other alloy (B) had a composition which had been investigated previously [5–8] and was selected for comparison.

## 2. Experimental details

The alloys $Pr_{20.5}Fe_{74.0}B_{3.5}Cu_{2.0}$ (A) and $Pr_{17.0}Fe_{76.5}B_{5.0}Cu_{1.5}$ (B) were investigated in the present study and were supplied by REP, Widnes, UK. The cast materials were annealed at 1000 °C in argon gas and then furnace cooled (250 °C $h^{-1}$) or quenched in liquid argon. Some samples were annealed in two steps: a first annealing at 1000 °C for 25 h and then a second annealing at 500 °C for varying times. The microstructures of the samples were examined using an optical microscope and a scanning electron microscope (SEM). The chemical compositions of the phases present in the samples were analysed by energy-dispersive X-ray (EDX) and/or wavelength-dispersive X-ray (WDX) spectroscopy in the SEM. Differential thermal analysis (DTA) studies were also carried out. The magnetic properties of the samples were measured using a permeameter (form of samples, $15 \times 15 \times 10$ $mm^3$) and a vibrating sample magnetometer (form of samples, $2 \times 2 \times 5$ $mm^3$).

## 3. Results and discussion

### *3.1. Metallographic studies*

Figure 1 shows the microstructures of the samples in the cast condition. The microstructure of alloy A consists of a $Pr_2Fe_{14}B$ matrix phase, praseodymium-rich grain boundary regions and free iron inside the matrix phase (Fig. 1(a)). In alloy B four phases — a $Pr_2Fe_{14}B$ matrix phase, praseodymium-rich grain boundary regions, a boron-rich phase (approximate composition $PrFe_4B_4$) and free iron inside the matrix phase — were observed (Fig. 1(b)). It is apparent that alloy A contains a larger amount of the praseodymium-rich grain boundary phase and exhibits a smaller grain size than alloy B. The smaller grain size of alloy A can be attributed to the higher copper and lower boron content. Copper additions to Pr–Fe–B-based alloys are known to reduce the grain size of the $Pr_2Fe_{14}B$ matrix phase [5] and the grain size is also reported to be coarsened with increasing boron content [9]. It is interesting to note that in alloy B a well-defined and fine eutectic morphology in the grain boundary regions is evident even in the cast state (Fig. 1(d)). No clear evidence for the presence of well-defined eutectic morphology is found in alloy A in the cast condition (Fig. 1(c)).

The annealed and quenched samples of both alloys show microstructures similar to those of the cast material (Figs. 2(a) and 2(b)). The eutectic morphology in the grain boundary region is more clearly visible in annealed

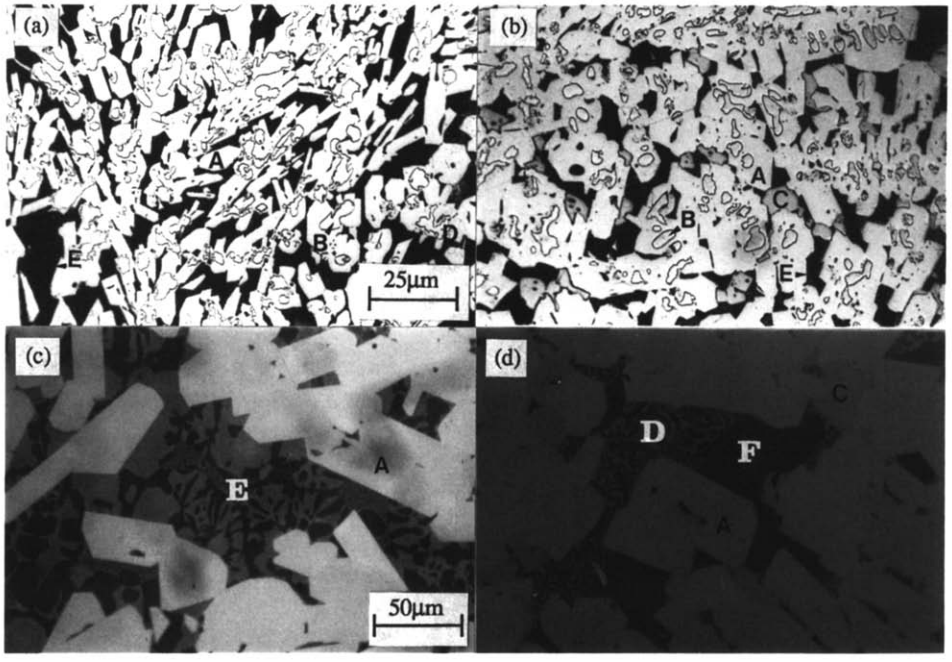


Fig. 1. Microstructures of alloys in cast condition (A, $Pr_2Fe_{14}B$; B, free iron; C, boride; D, eutectic; E, praseodymium rich; F, primary praseodymium rich): (a) alloy A (etched); (b) alloy B (etched); (c), (d) close examinations of grain boundary regions in alloys A and B (unetched) respectively.

and furnace-cooled samples of both alloys as shown in Figs. 2(c) and 2(d). The grain boundary region in the furnace-cooled samples of both alloys consists of the primary praseodymium-rich phase and the eutectic phases. Microanalysis results show that the eutectic phase region is enriched in copper (see Table 1). In particular, the light phase in the eutectic region was found to be very rich in copper. The copper contents in the light and dark phases in the eutectic region are found to be around 34.0 and 4.0 at.% respectively. In contrast, the copper content in the primary praseodymium-rich phase is found to be very low (around 0.3 at.%). The compositions of the phases common to both alloys appeared to be essentially the same. In both alloys the free iron observed in the matrix phase in the cast material was removed by annealing and it was also found that the free iron was removed more rapidly in alloy A (5 h) than in alloy B (20 h). The more rapid removal of the free iron in alloy A is probably due to the smaller grain size and the greater amount of praseodymium-rich grain boundary phase. The grain boundary eutectic becomes liquid at the high annealing temperature and therefore acts as an effective diffusion path. Thus the presence of a greater amount of liquid phase facilitates the diffusion of the constituent atoms through it and this contributes to the rapid removal of the free iron in alloy A.

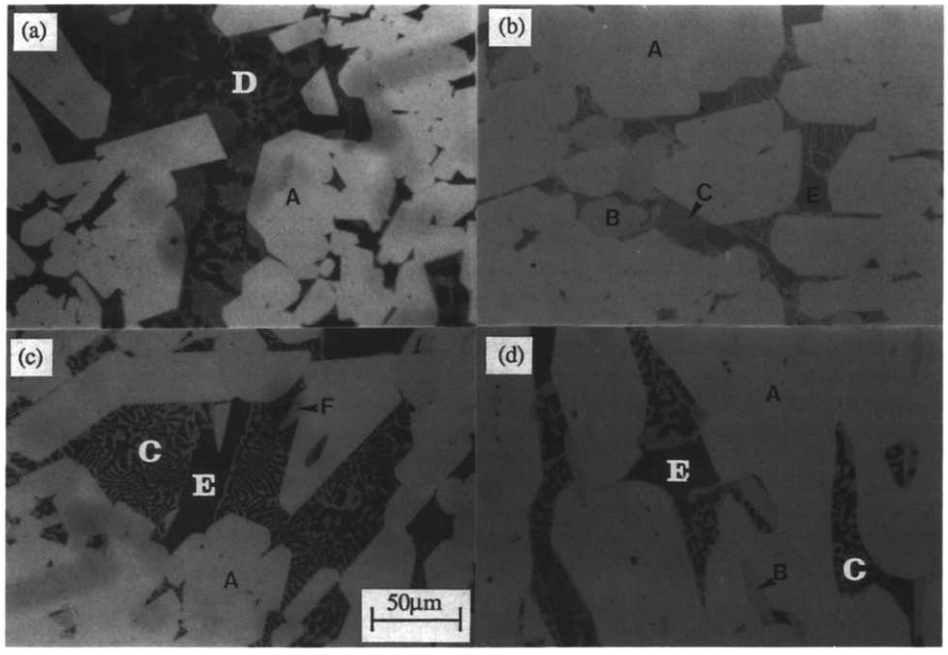


Fig. 2. Microstructures of alloys quenched or furnace cooled after annealing (unetched) (A, $Pr_2Fe_{14}B$; B, boride; C, eutectic; D, praseodymium rich; E, primary praseodymium rich; F, $PrFe_2$ type): (a) alloy A (quenched); (b) alloy B (quenched); (c) alloy A (furnace cooled); (d) alloy B (furnace cooled).

TABLE 1

Chemical compositions of phases in atomic per cent (error ±1.0)

| Phase | | Pr | Fe | B | Cu | Method |
|---|---|---|---|---|---|---|
| Primary Pr rich | | 96.3 | 1.1 | 2.3 | 0.3 | WDX+ EDX |
| Eutectic | dark[a] | 93.1 | 2.9 | | 4.0 | EDX |
| | light[a] | 63.1 | 2.9 | | 34.0 | EDX |
| Needle like | | 32.3 | 62.5 | 1.1 | 4.1 | WDX+EDX |

[a]Based on assumption of zero boron content.

Examination of the microstructure of alloy A in the furnace-cooled condition indicates the presence of a grey phase in the grain boundary regions (see Fig. 2(a)). The presence of this phase is more evident in the sample which was subjected to a post-annealing treatment at the lower temperature of 500 °C (Fig. 3(a)), which is just above the melting point of the eutectic (see Fig. 4). A very fine eutectic was observed in the dark regions shown in Fig. 3(a), but this is not visible in the photograph owing to the air-etching procedure. No evidence for the presence of the grey phase was found in alloy B (Fig. 3(b)). The chemical composition of this phase is given in Table

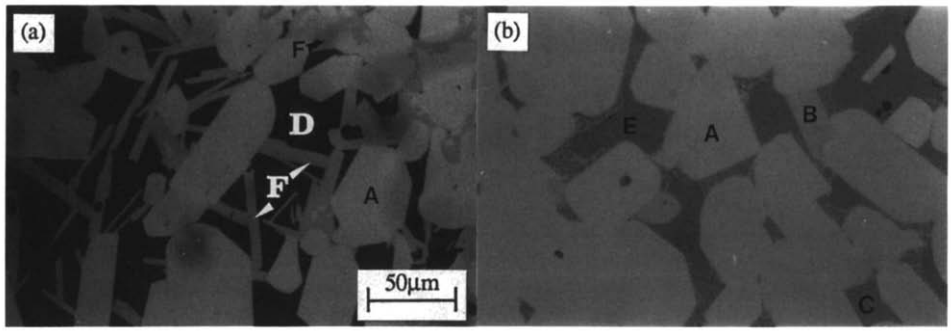


Fig. 3. Microstructures of alloys post-annealing treated at low temperature (first annealing at 1000 °C for 20 h and then quenching; second annealing at 500 °C for 7 h and then quenching) (A, $Pr_2Fe_{14}B$; B, boride; C, eutectic; D, praseodymium rich; E, primary praseodymium rich; F, $PrFe_2$ type): (a) alloy A (air etched); (b) alloy B (unetched).

TABLE 2

Grain boundary characteristics of alloys

| Condition | Alloy | Boride | Eutectic | $PrFe_2$ type | Primary Pr rich |
|---|---|---|---|---|---|
| As-cast | A | No | Not evident | No | Yes |
| | B | Yes | Well defined | No | Yes |
| Annealing + quenching | A | No | Not evident | No | Yes |
| | B | Yes | Well defined | No | Yes |
| Annealing + furnace cooling | A | No | Evident | A little | Yes |
| | B | Yes | Well defined | No | Yes |
| Two-step annealing | A | No | Fine | Considerable | Yes |
| | B | Yes | Well defined | No | Yes |

1 and it is found that the ratio Pr:(Fe+Cu) is about 1:2. This phase may possibly be related to a $PrFe_2$-type Laves phase, but such a phase does not exist under equilibrium conditions and it has been reported [10] that the $PrFe_2$ phase can be formed only at high temperature and under high pressure in the Pr–Fe binary system. The extra phase may therefore be stabilized by the presence of Cu and/or B atoms. The grain boundary characteristics of the alloys in various conditions are summarized in Table 2.

Figure 4 shows the results of the DTA studies. The Curie temperature of the matrix phase in both alloys and the melting point of the grain boundary eutectic were found to be around 280–290 and 450 °C respectively.

### *3.2. Magnetic measurements*

#### *3.2.1. Effect of annealing on magnetic properties*

Variations in the intrinsic coercivity of both alloys as a function of the annealing time at 1000 °C for the quenched or furnace-cooled samples are shown in Fig. 5. The intrinsic coercivities of alloy A are consistently higher

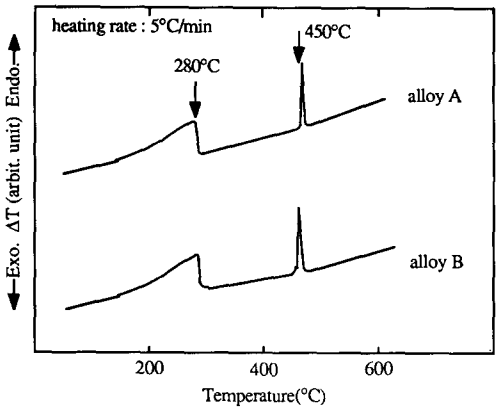


Fig. 4. DTA results for fully annealed alloys.

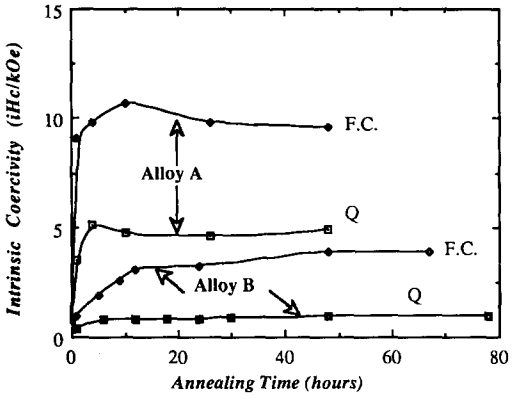


Fig. 5. Variations in intrinsic coercivity as a function of annealing time at 1000 °C (F.C., furnace cooled; Q, quenched).

than those of alloy B. The higher intrinsic coercivity of alloy A can be attributed to its smaller grain size and greater amount of grain boundary phase. Thus the matrix phase grains are well isolated from one another, which reduces the magnetic coupling between them and therefore enhances the intrinsic coercivity.

Figure 5 shows that for both the quenched and the furnace-cooled samples there is a more rapid improvement in the intrinsic coercivity in alloy A compared with that in alloy B. As discussed earlier, the presence of the greater amount of grain boundary phase in alloy A, which is liquid at the annealing temperature, probably facilitates the diffusion of the constituent atoms and thus the free iron inside the matrix (see Fig. 1(a)) can be removed more easily. The improvement in the intrinsic coercivity in the annealed and quenched samples compared with the cast samples (particularly alloy A) can also be attributed to the removal of free iron during the annealing treatment.

No significant improvement in the intrinsic coercivity was achieved in the alloy B samples after annealing and quenching.

Although the free iron was removed completely in alloy B by prolonged annealing (20 h at 1000 °C), the magnetic separation between the matrix grains may not be sufficient owing to the lack of grain boundary phase, thus resulting in the poor intrinsic coercivity.

It can be seen that the furnace cooled samples show substantially higher intrinsic coercivities than the quenched samples. This may be attributed to the smoothing of the grain boundary surface of the matrix phase during the furnace cooling. Thus solid–liquid reaction between the matrix grains and the grain boundary liquid phase during furnace cooling may result in the smoothing of the grain boundary surface, thus significantly reducing the number of possible sites for reverse domain nucleation and hence enhancing the intrinsic coercivity. Quenching, on the other hand, could produce irregularities at the boundary [11].

Another possibility, not mutually exclusive, is that the quenching treatment results in constitutional changes (probably in the praseodymium-rich phase) at the grain boundaries which degrade the coercivity.

Figure 6 shows typical demagnetization curves of the cast alloys and the annealed alloys in the state showing optimum magnetic properties. In Table 3 the peak magnetic properties of the alloys obtained by furnace cooling following high temperature annealing are shown. Alloy A shows much

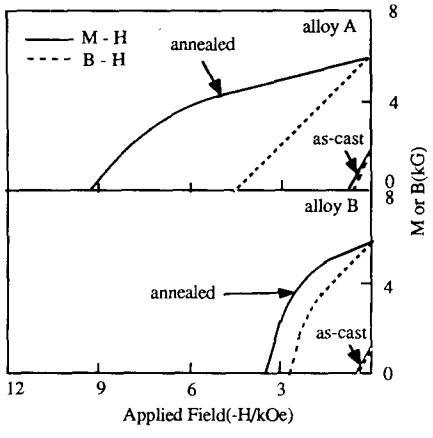


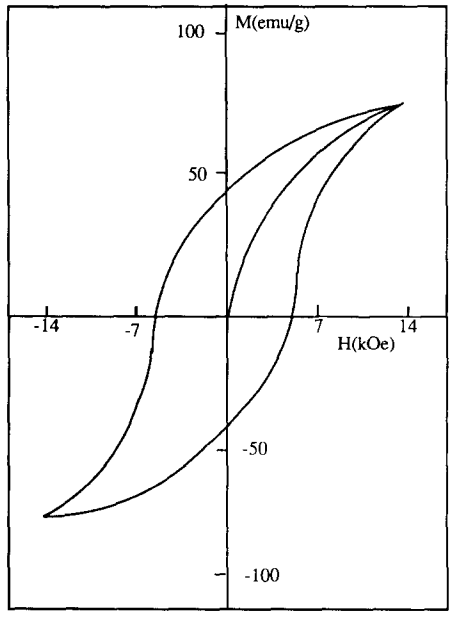


Fig. 6. Demagnetization curves of as-cast and fully annealed samples.

Fig. 7. Typical minor hysteresis loop and initial magnetization curve of fully annealed alloy A.

TABLE 3

Peak magnetic properties of alloys

| | $iH_c$ (kOe) | $B_r$ (kG) | $(BH)_{max}$ (MG Oe) |
|---|---|---|---|
| Alloy A | 10.7 | 6.1 | 7.6 |
| Alloy B | 3.9 | 5.8 | 4.8 |

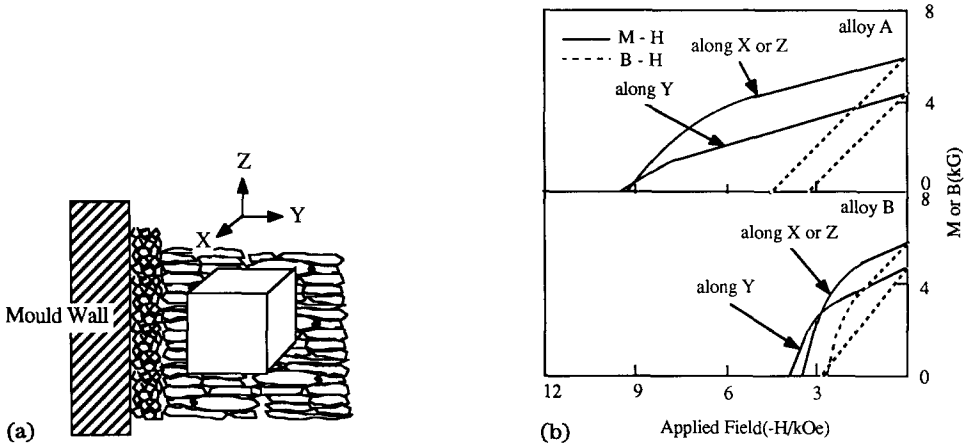


Fig. 8. Demagnetization curves of fully annealed alloys measured along different directions: (a) schematic diagram showing measuring directions; (b) demagnetization curves along different directions.

better permanent magnetic properties compared with those of alloy B when subject to the same treatments.

A typical minor hysteresis loop and initial magnetization curve measured by the vibrating sample magnetometer for the annealed and the furnace-cooled alloy A sample are shown in Fig. 7 (uncorrected for the demagnetizing factor of the sample). The initial magnetization curve is consistent with a typical nucleation-type coercivity mechanism. The furnace-cooled alloy B sample also showed a similar initial magnetization behaviour. Figure 8 shows typical demagnetization curves of the alloys in the condition showing optimum magnetic properties; the demagnetization curves were measured along different directions in the ingot. Remanence is significantly higher in the *X* and *Z* directions (particularly in alloy A), which indicates some preferred orientation with preferred radial *c*-axis alignment within the *XZ* plane.

*3.2.2. Effect of step annealing on magnetic properties*

In order to investigate more thoroughly the changes in the intrinsic coercivity on annealing, samples were also subjected to a two-step annealing procedure. Samples were first annealed at 1000 °C for 25 h and quenched. The quenched samples were then re-annealed at the lower temperature of

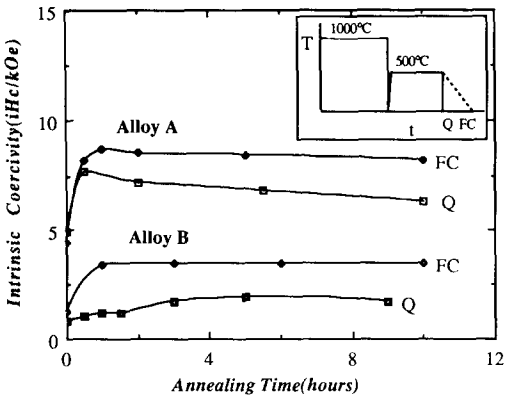


Fig. 9. Variations in intrinsic coercivity as a function of annealing time at 500 °C; samples were initially aged at 1000 °C for 25 h and then quenched (F.C., furnace cooled; Q, quenched).

500 °C. The annealed samples were then quenched or furnace cooled from 500 °C and the variations in the intrinsic coercivity as a function of annealing time at the lower temperature are shown in Fig. 9. The inset in Fig. 9 shows the heat treatment profile used in the two-step annealing treatment. These results indicate that the lower temperature annealing treatment improves the coercivity values of both alloys when compared with the samples annealed at 1000 °C and quenched (Fig. 5). This could be due to the improvement in the surface character of matrix grains during annealing at the lower temperature. It is worth noting that the presence and form of the Pr(Fe, $Cu)_2$ phase observed in the two-step aged alloy A (see Fig. 3(a)) may influence the coercivity behaviour of the material. The precise effect of this phase on the intrinsic coercivity is not well understood at the present time and more detailed study is required. It should be noted that recent work [12–14] in this laboratory on sintered magnets based on the alloy Nd–Fe–B–Cu has shown that a phase with composition around $Nd_{30}Fe_{65}Cu_5$ appears to play a vital role in improving the coercivity of these magnets on annealing at 600 °C.

## 4. Conclusions

Alloy A ($Pr_{20.5}Fe_{74.0}B_{3.5}Cu_{2.0}$) was found to contain greater amounts of the grain boundary phase and to have a smaller grain size than alloy B ($Pr_{17.0}Fe_{76.5}B_{5.0}Cu_{1.5}$). The microstructure of alloy A consisted of a $Pr_2Fe_{14}B$ matrix phase, a praseodymium-rich grain boundary phase and free iron inside the matrix phase in the cast condition. In alloy B, in addition to the above three phases, the $PrFe_4B_4$ phase (approximate composition) was also observed. On annealing at 1000 °C followed by furnace cooling, a binary eutectic was observed clearly in the grain boundary regions in alloy A. Alloy B exhibited a clear eutectic even in the cast state. The eutectic phase region was found

to be copper-rich. In particular, the light phase in the eutectic region was significantly enriched in copper. An extra phase was observed in alloy A in the fully annealed condition and X-ray microanalysis results indicated that it is a Pr(Fe, $Cu)_2$-type phase. Much better permanent magnetic properties were achieved in alloy A. This has been attributed to a smaller grain size and better magnetic isolation between the magnetic phase grains due to the presence of a greater amount of grain boundary phase. Furnace cooling following annealing at high temperature leads to higher intrinsic coercivity than on quenching, which could be due to the improvement in the surface character (smoothness) of the magnetic phase grain boundary during the furnace cooling and/or to constitutional changes in the grain boundary material. The magnetic properties indicated some preferred orientation in both alloys in the cast state, particularly in the case of alloy A.

## Acknowledgments

Thanks are due to the SERC and CEAM for the provision of research grants, to REP for the provision of alloys (in particular G. Mycock) and to N. A. Smith for help with the DTA measurements.

## References

1 M. Q. Huang, E. Oswald, E. B. Boltich, S. Hirosawa, W. E. Wallace and E. Schwab, *Physica B, 130* (1985) 319.
2 E. B. Boltich and W. E. Wallace, *Solid St. Commun., 55* (1985) 529.
3 S. Hirosawa, Y. Matsuura, H. Yamamoto, S. Fujimura, M. Sagawa and H. Yamauchi, *J. Appl. Phys., 59* (1986) 873.
4 F. Pourarian, S. Simizu, R. T. Obermyer, S. G. Sankar and W. E. Wallace, *Proc. 11th Int. Workshop on Rare-earth Magnets and Their Applications, Pittsburgh, PA, 1990, p. 401.*
5 T. Shimoda, K. Akioka, O. Kobayashi and T. Yamagami, *J. Appl. Phys., 64* (1988) 5290.
6 G. C. Hadjipanayis, M. Zhang and C. Gao, *Appl. Phys. Lett., 54*(18) (1989) 1812.
7 T. Shimoda, K. Akioka, O. Kobayashi, T. Yamagami and A. Arai, *Proc. 11th Int. Workshop on Rare-earth Magnets and Their Applications, Pittsburgh, PA, 1990,* p. 17.
8 H. W. Kwon, P. Bowen and I. R. Harris, *J. Appl. Phys., 70*(10) (1991) 6357.
9 C. R. Paik, H. Nakamura, M. Okada and M. Homma, *Proc. 10th Int. Workshop on Rare-earth Magnets and Their Applications, Kyoto, 1989,* p. 631.
10 J. F. Cannon, *Mater. Res. Bull., 7* (1972) 5.
11 M. Sagawa and S. Hirosawa, *J. Phys. (Paris), 49* (1988) 617.
12 A. Kianvash and I. R. Harris, *J. Appl. Phys., 70* (10) (1991) 6453.
13 G. Knoch, A. Kianvash and I. R. Harris, *J. Alloys Comp.*, in press.
14 A. Kianvash and I. R. Harris, *J. Alloys Comp., 178* (1992) 325–341.